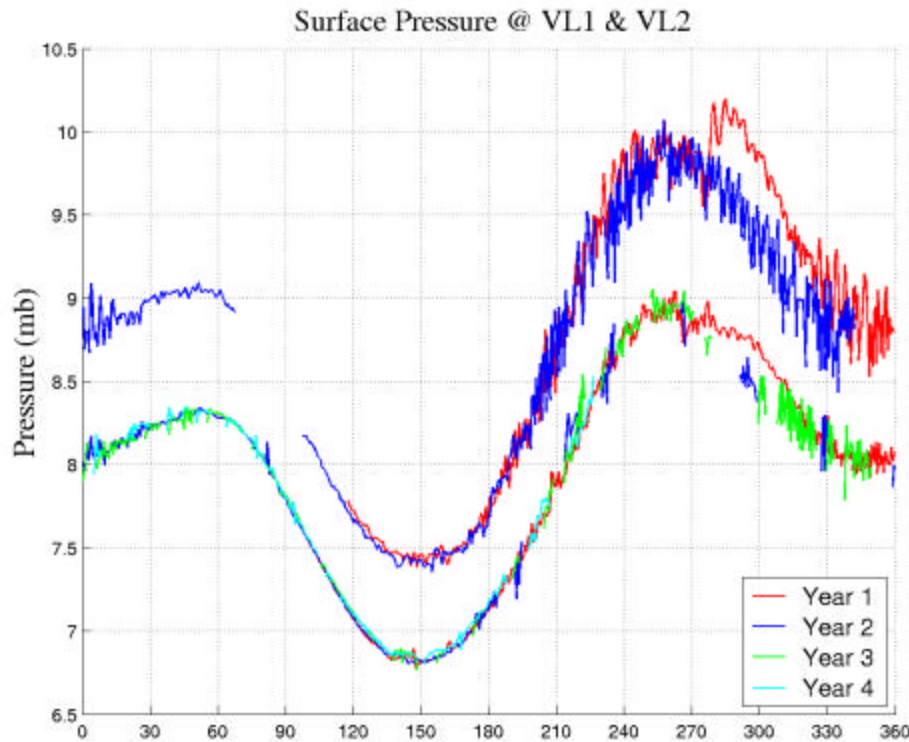


A Comparison of Thermal Tides and Propagating Waves in Mars GCMs



Participating Models:

Ames
GFDL
Japan
LMD
Oxford

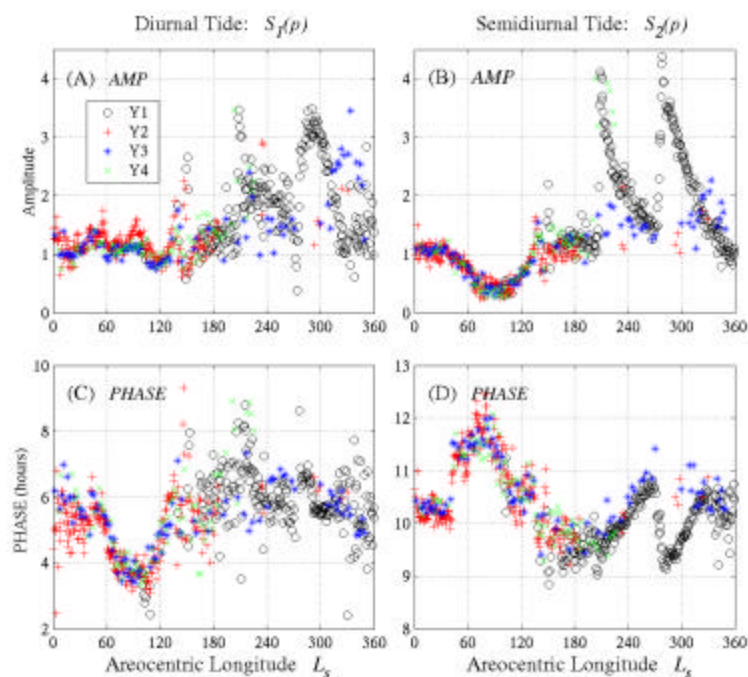
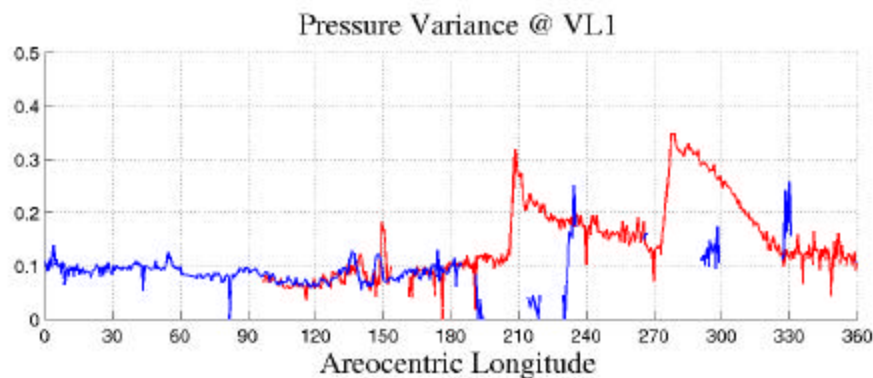
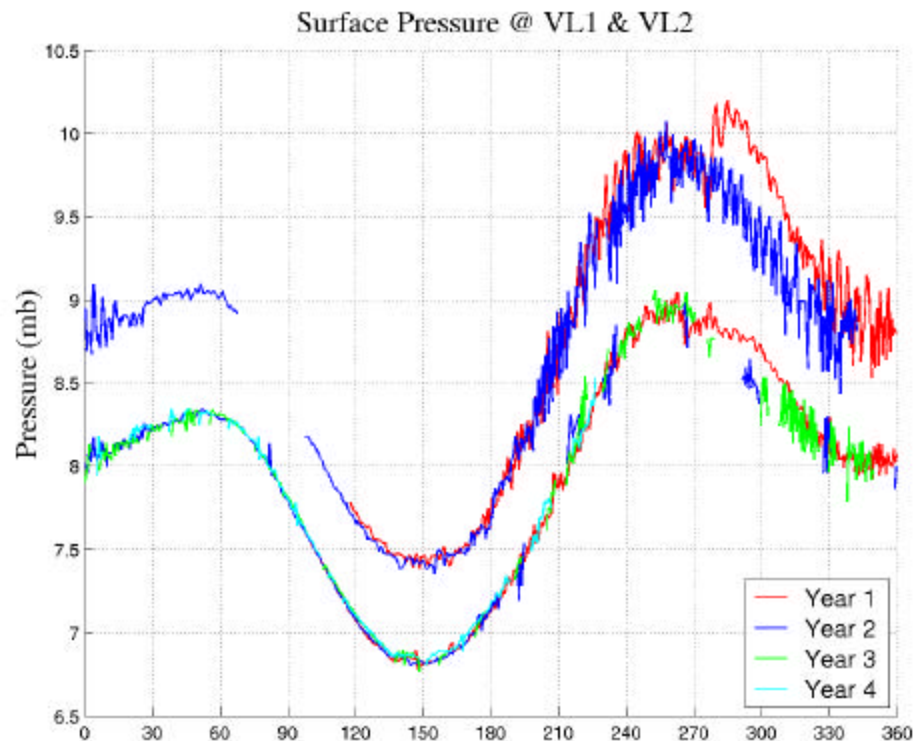
Viking Lander Surface Pressure Data

VL1 & VL2

CO₂ Condensation Cycle

Traveling Waves

Thermal Tides



Tides

- Evaluate effective thermal forcing due to heat fluxes from the surface into the boundary layer, and to dust heating
- Look for commonality in the simulated excitation of nonmigrating tides to provide insight for interpreting observed surface pressure tides at landed meteorological stations.

Traveling Waves:

Look for patterns and commonality in the seasonal evolution of traveling waves, and the possible dependence on atmospheric opacity.

Compare the signatures of traveling waves in surface pressure and air temperature at various levels.

Examined P_{sfc} T_{15} and $T_{2\text{km}}$ fields for 1 Mars year (668 sols), with good diurnal sampling (12-24x/sol)

Examined 19 Simulations:

Ames: $\tau = 0.0, 0.3, 1.0$

GFDL: $\tau = 0, 0.15, 0.3, 1.0$, and 0.3^*

Japan: $\tau = 0, 0.3$, “Viking”

LMD: $\tau = 0.0, 0.2$, MGS, 2.0

Oxford: $\tau = 0.0, 0.2, 0.3$, Viking

Data Processing

Removed annually-varying trend (periods > 30 sols) at each model gridpoint

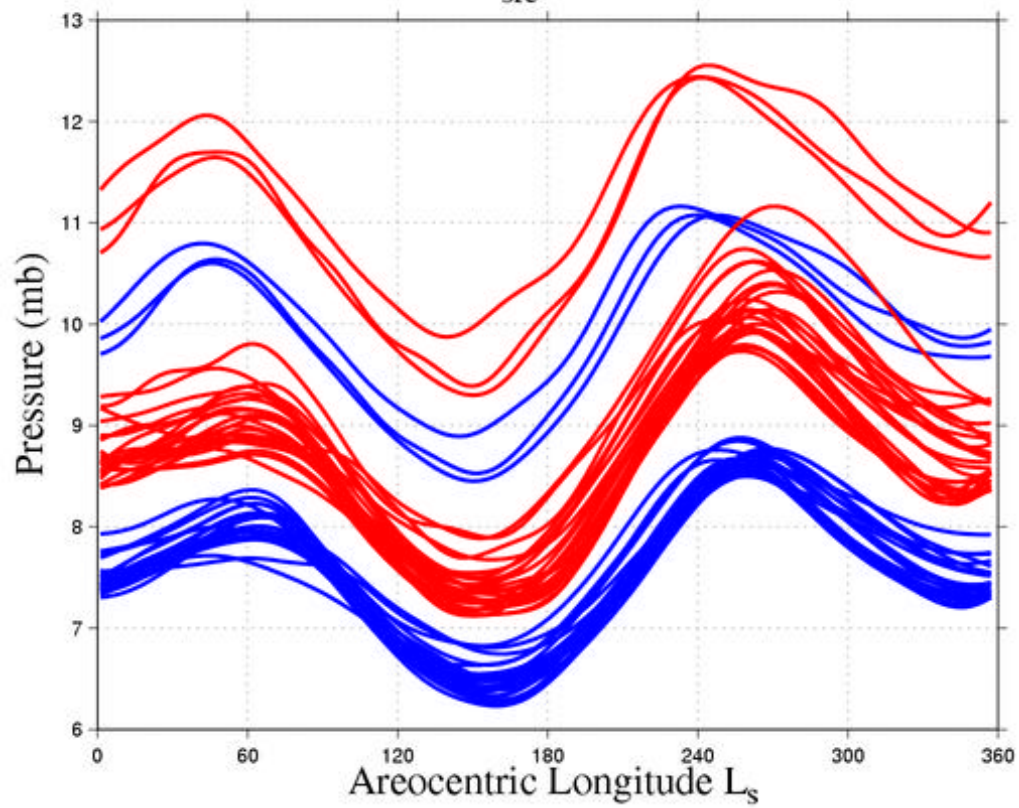
Tides:

- Calculated the diurnal and semidiurnal harmonics of P_{sfc} at each gridpoint (5 sol composites). In particular, VL and Pathfinder sites are thus represented.
- Space-Time spectral-decomposition of the pressure fields yielding seasonal evolution of Eastward and westward propagating zonal waves ($s=1-4$) with diurnal and semidiurnal harmonics:

Traveling waves:

- Band-pass filtered data: retained periods between 1 and 30 sols. Computed variance of P_{sfc} and T at each gridpoint.
- Space-Time spectral-decomposition of field, using overlapping 60-sol periods to capture seasonal evolution of eastward and westward propagating zonal waves 1-4
- Computed Empirical Orthogonal functions (EOF's) for both NH and SH variability.

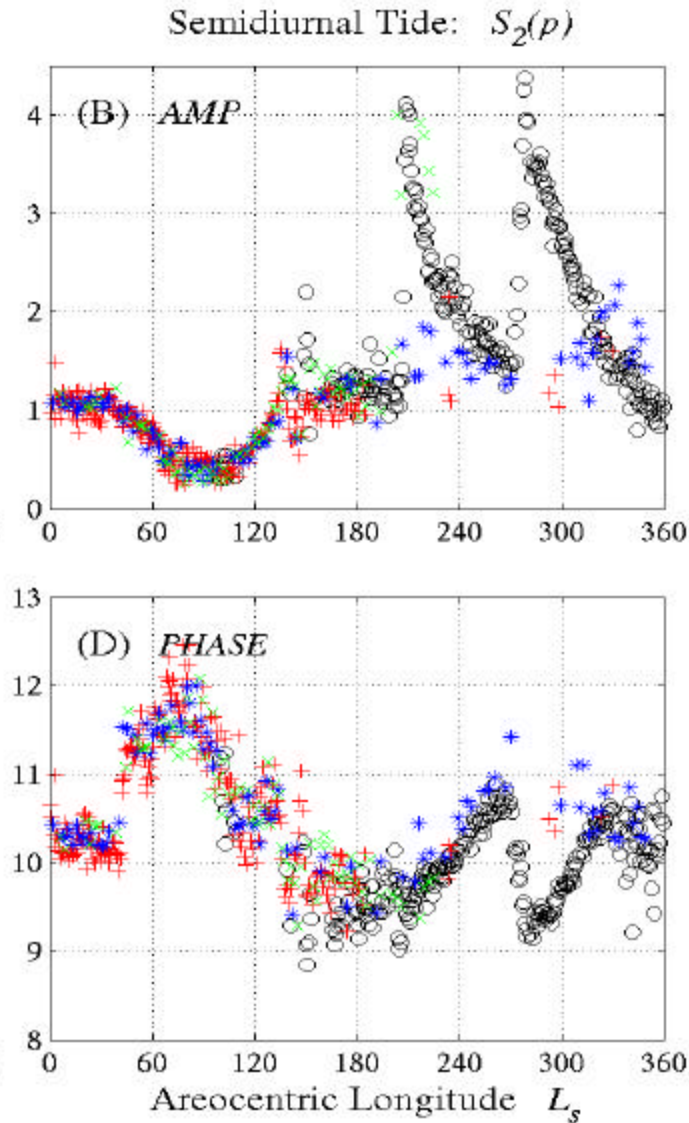
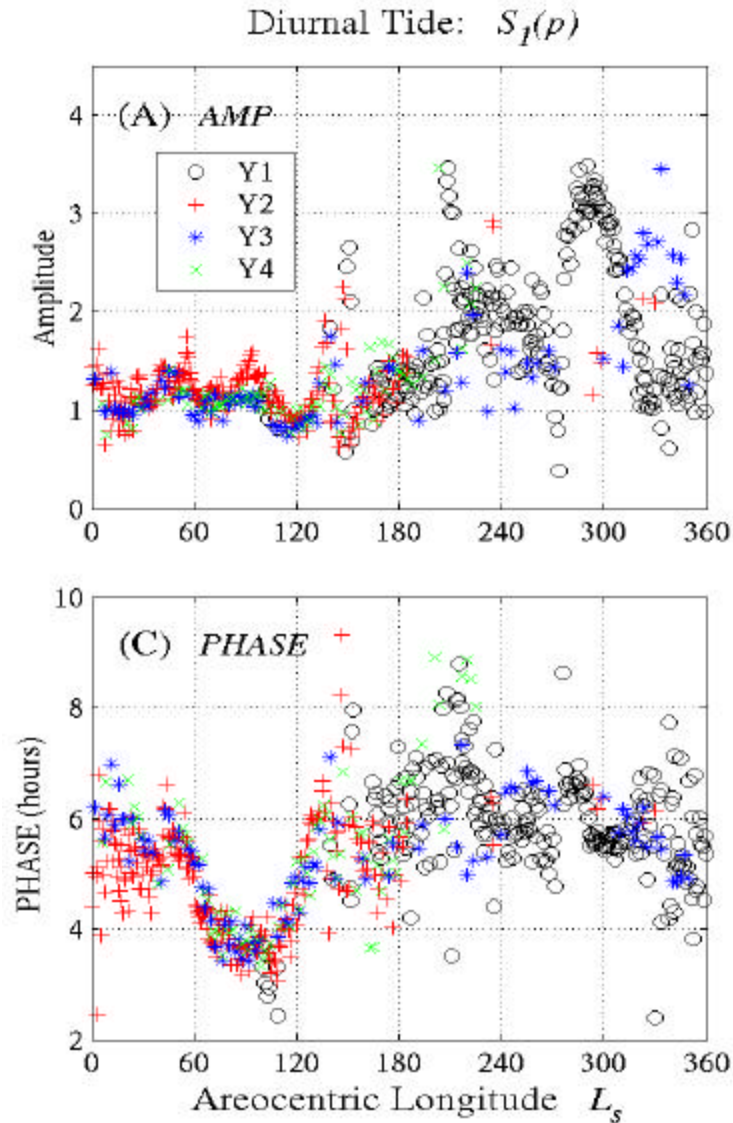
Simulated P_{sfc} at VL1 and VL2



Diurnal and Semidiurnal Surface Pressure Oscillations at VL1 (22° N)

4 Year record

$$\text{Amp} = P_{\text{tide}} / P_{\text{diavg}}$$



High degree of
regularity in the
 $L_s=0-180$ period

Semidiurnal Tide $S_2(p)$:

Sun-synchronous component:

Dominated by single Hough mode

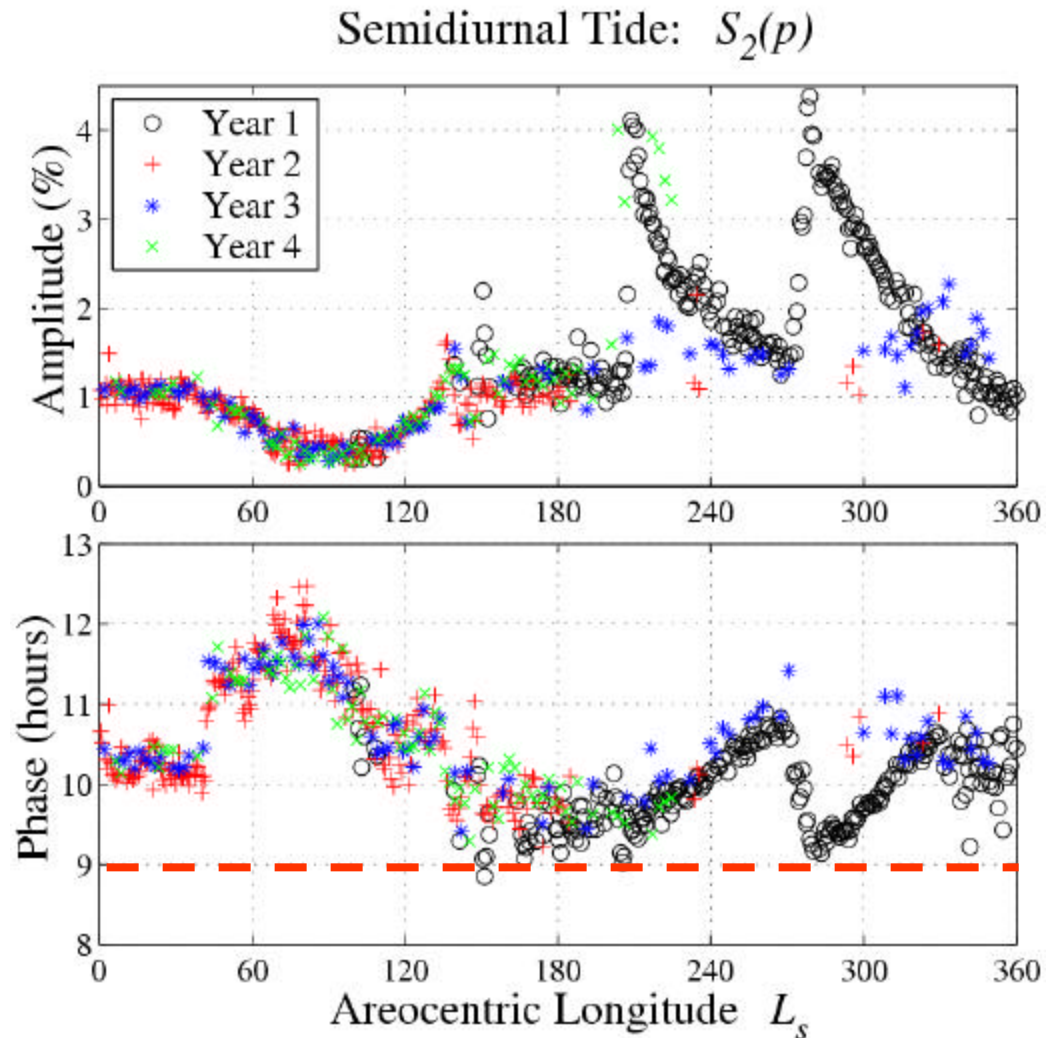
- Broad meridional structure
- Very deep vertical structure

Therefore $S_2(p)$ is the integrated response of atmospheric heating

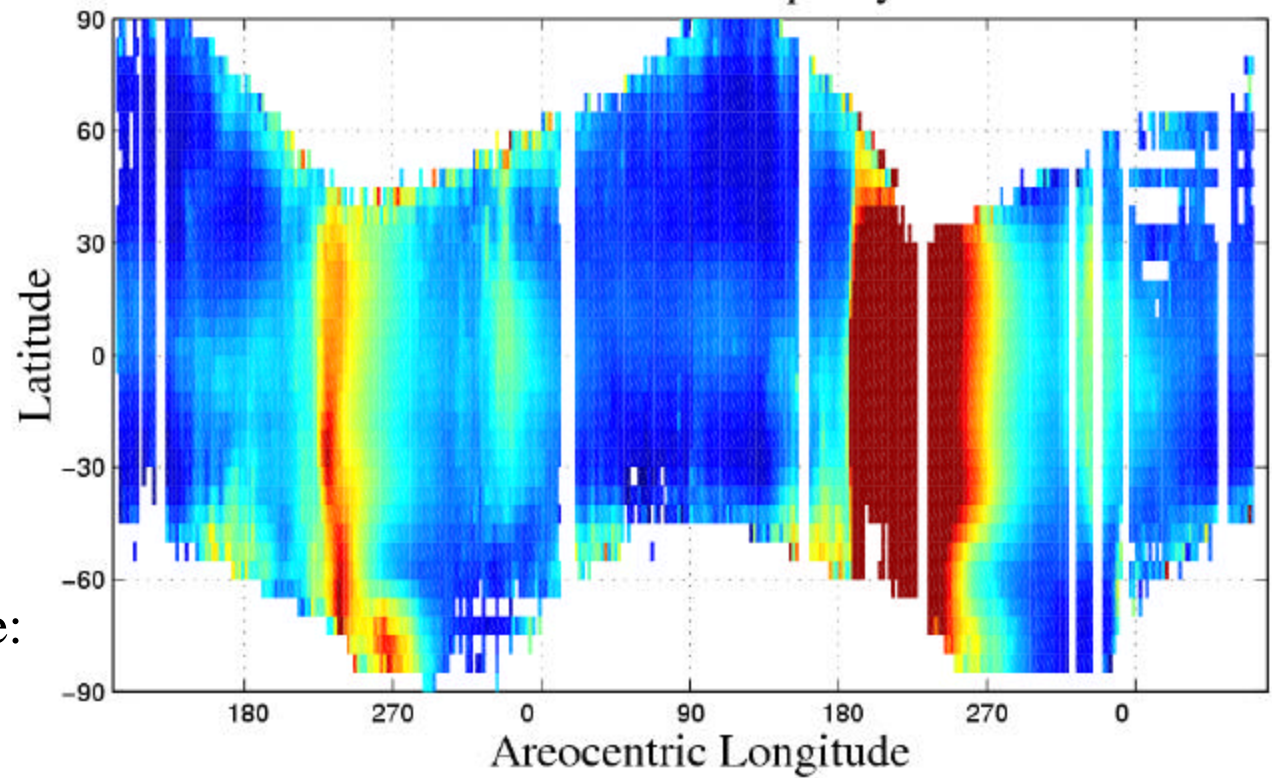
Phase \sim 0900 LT

This mode should be dominant during particularly dusty periods.

Departure in Phase from 0900 LT due to nonmigrating tides

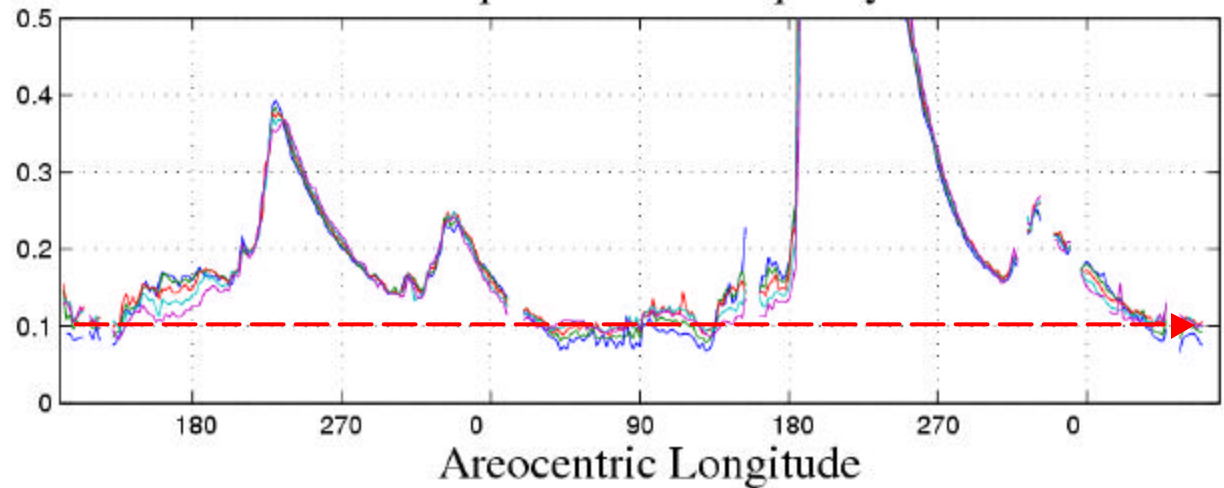


TES IR Dust Opacity



Opacity Color Range:
0 to 0.5

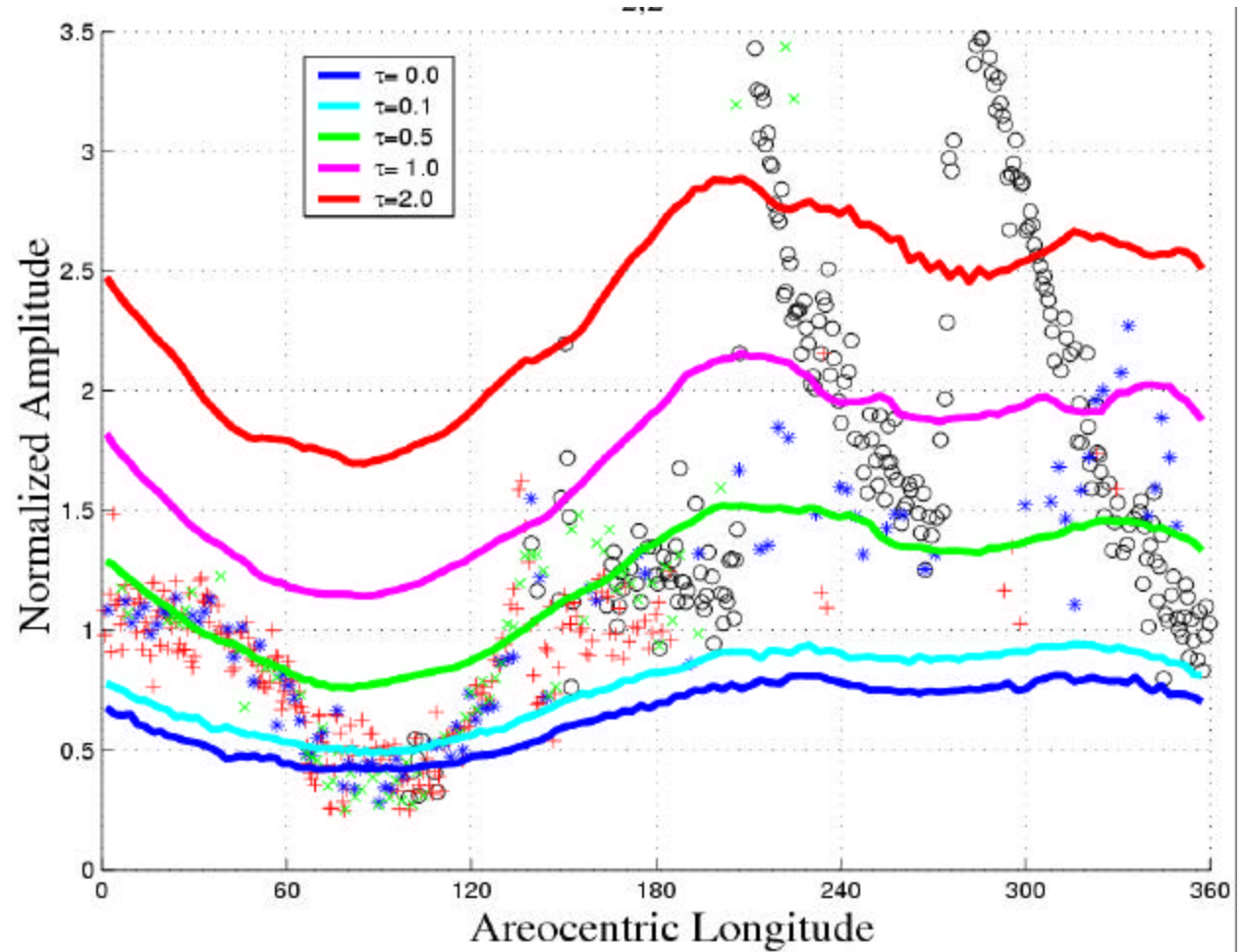
Tropical IR Dust Opacity



Uniform
background dust for
 $L_s=40-140^\circ$

Opacities provided by
Mike Smith, GSFC

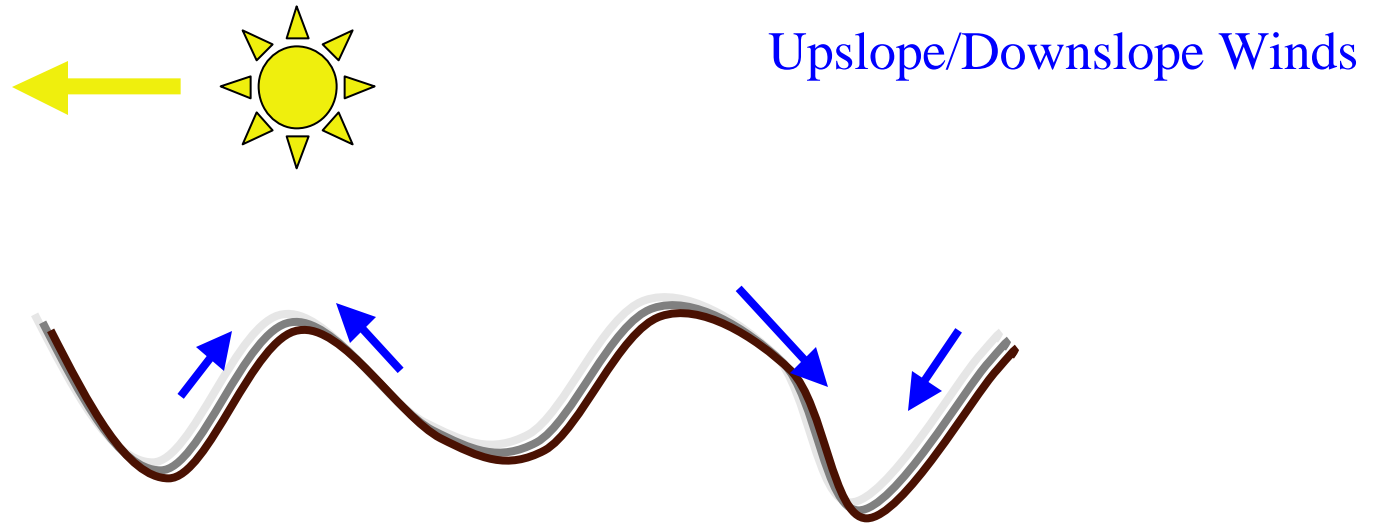
Simulated Migrating Component of $S_2(p)$ 22°N



VL1 response due to sun-synchronous tide + nonmigrating tide components: Kelvin wave is particularly strong during NH Summer solstice.

Nonmigrating tide: zonal modulation of the sun-synchronous tide by topography etc.

Migrating tides are scattered into nonmigrating tides



$$\cos[\mathbf{s}\hat{\lambda} + \mathbf{s}t] \cos [m\hat{\lambda}] = \cos[(\mathbf{s} + m)\hat{\lambda} + \mathbf{s}t] + \cos[(\mathbf{s} - m)\hat{\lambda} + \mathbf{s}t]$$

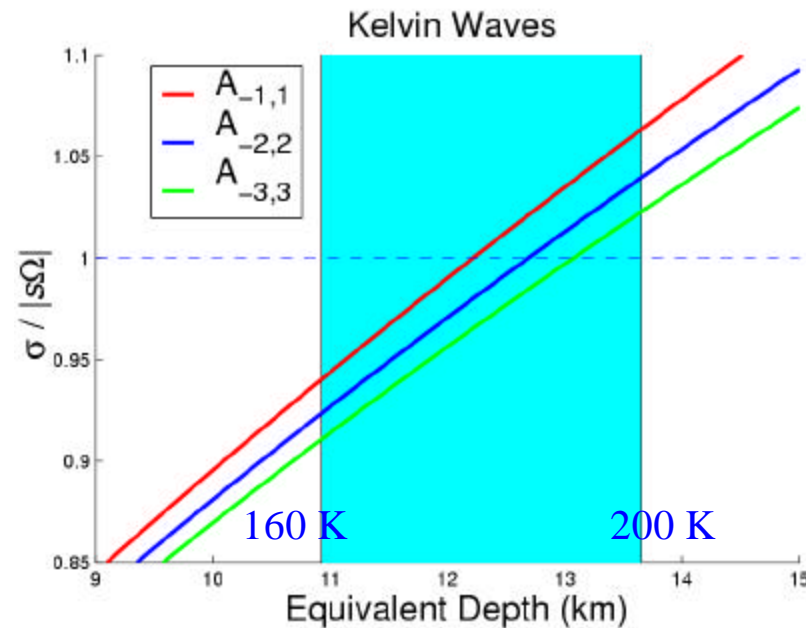
Wave 2 Topography: $\cos[\lambda - t]$ eastward propagating diurnal wave

Wave 4 Topography: $\cos[2\lambda - 2t]$ eastward propagating semidiurnal wave

Other tide modes are generated as well, will ignore for now

Relevant for vertically propagating response

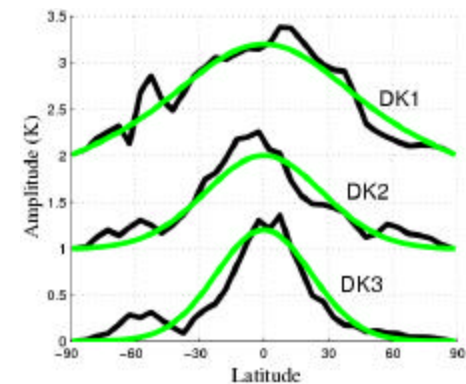
Resonant Kelvin Waves



Eastward Propagating

Meridionally Broad

Barotropic Vertical structure



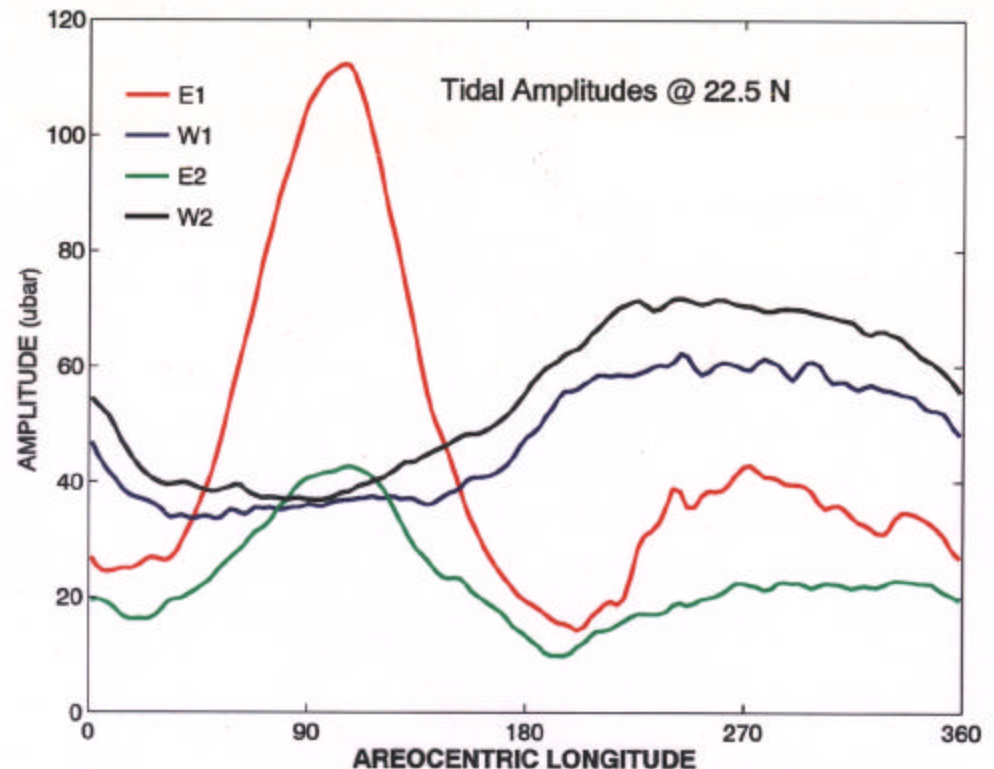
External Mode Equivalent Depth: $h_{\text{res}} = H/(1-\kappa)$

Resonant response by the Diurnal and Semidiurnal Kelvin waves

Resonant enhancement of the **diurnal Kelvin** wave (**E1**) at $L_s = 90$

Weaker enhancement of the **semidiurnal Kelvin** wave (**E2**)

More uniform variation in the migrating tides, (**W1** & **W2**) due to seasonal variations in insolation



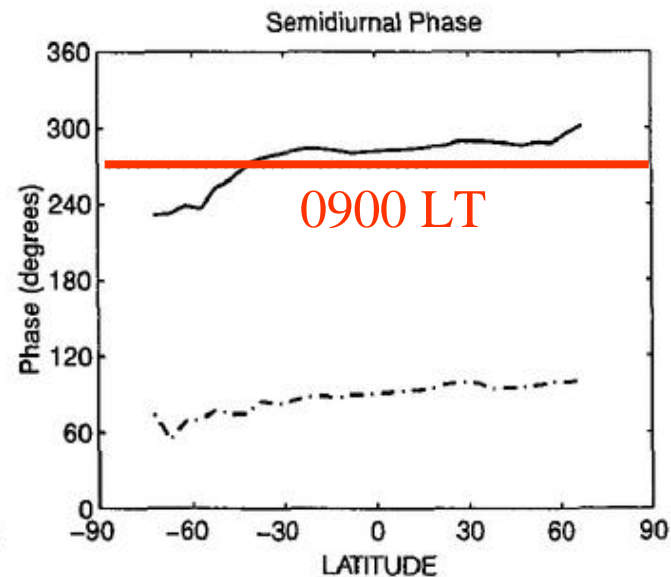
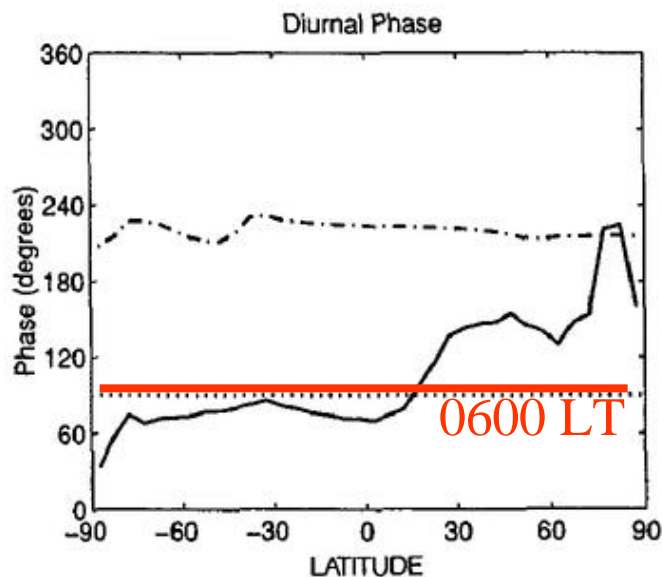
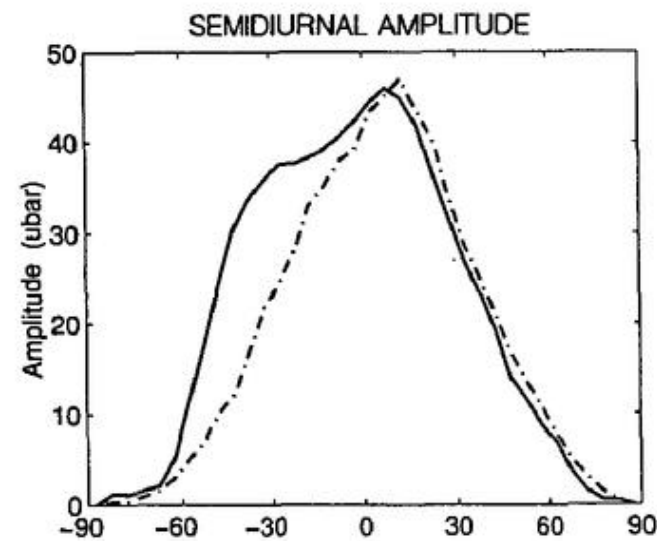
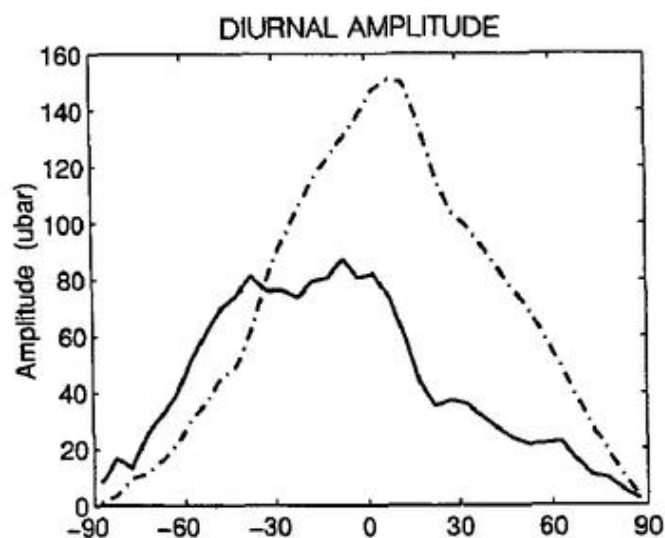
MGCM Simulation: $L_s = 90^\circ$

Eastward and Westward propagating components

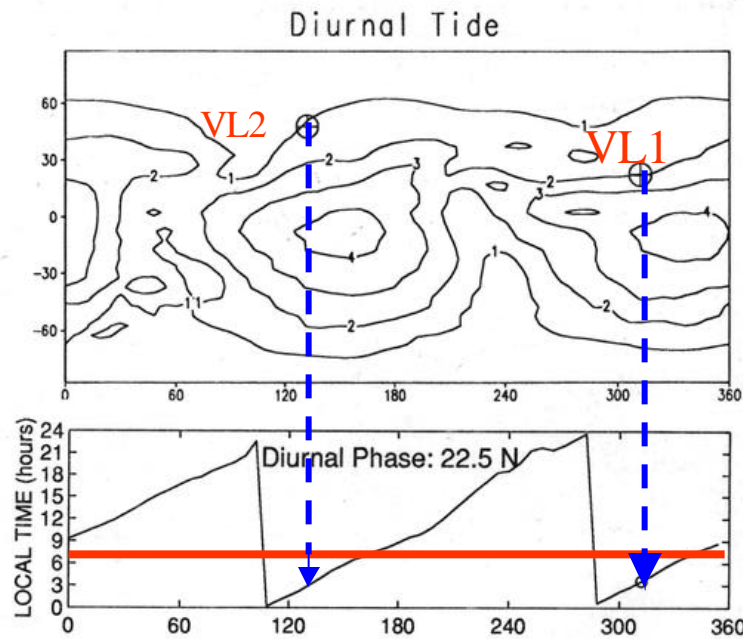
Westward —
Eastward ----

$A_{-1,1}$ and $A_{-2,2}$
are
resonantly
enhanced in
this season

Phase
determined by
resonance and
forcing

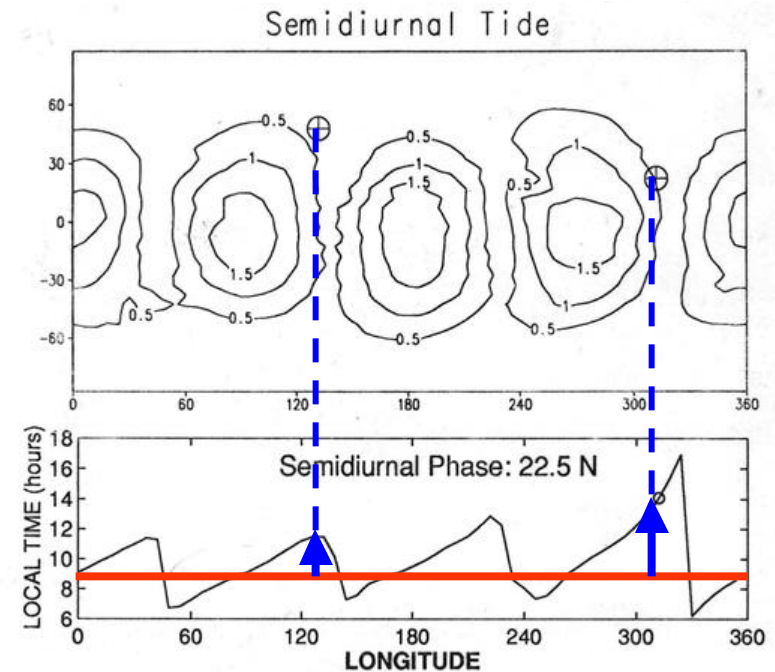


Simulated Surface Pressure Amplitude and Phase : $L_s \sim 90^\circ$



Wave 2 Interference Pattern

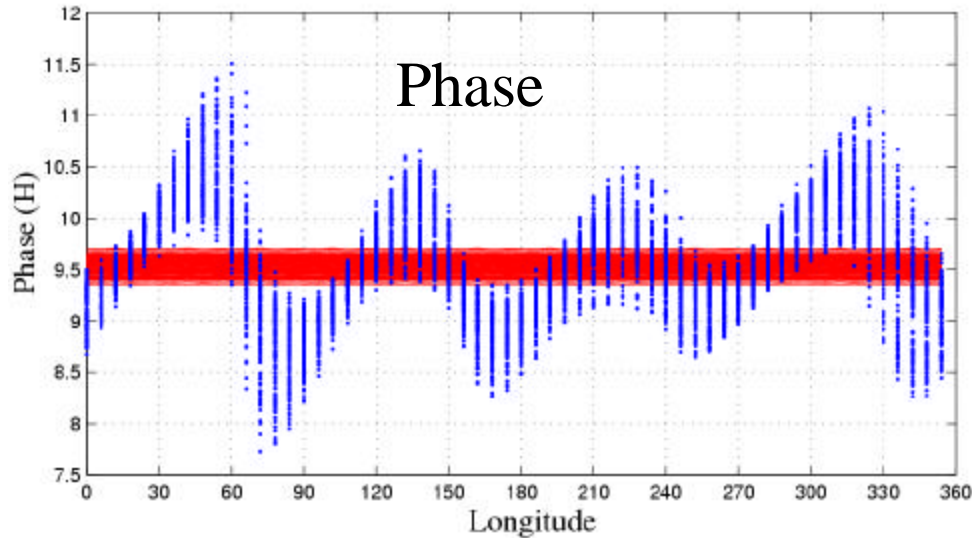
- $A_{1,1}$ & $A_{-1,1}$ modes dominant
- Simultaneous Phase Advance at two lander sites for diurnal tide as $A_{-1,1}$ increases – As observed



Wave 4 Interference Pattern

- $A_{2,2}$ & $A_{-2,2}$ modes dominant
- Simultaneous Phase Delay for Semidiurnal tide as $A_{-2,2}$ increases- As observed

Semidiurnal Tide (22°N): Envelope of Seasonal Variation

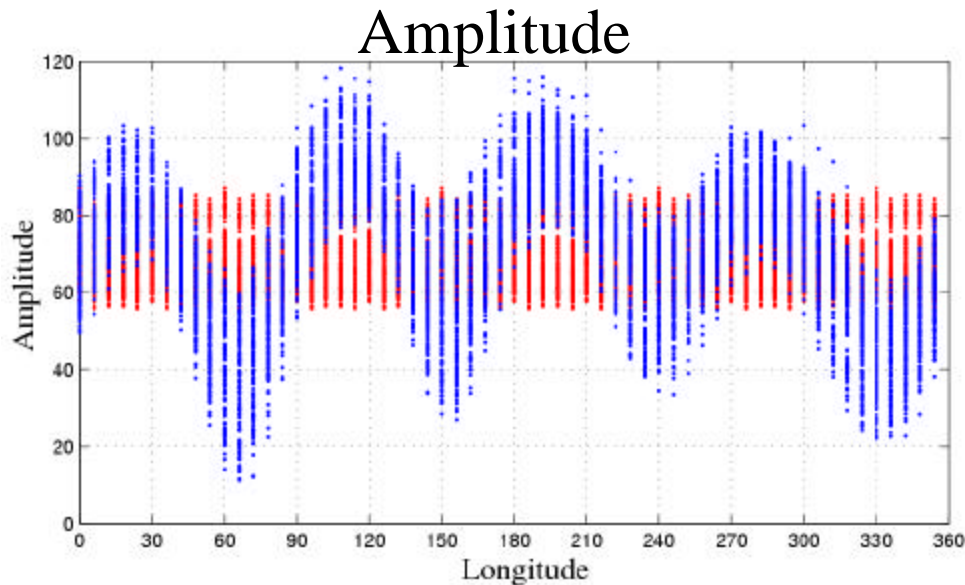


Fixed Dust simulation:

Local Tide

Migrating component

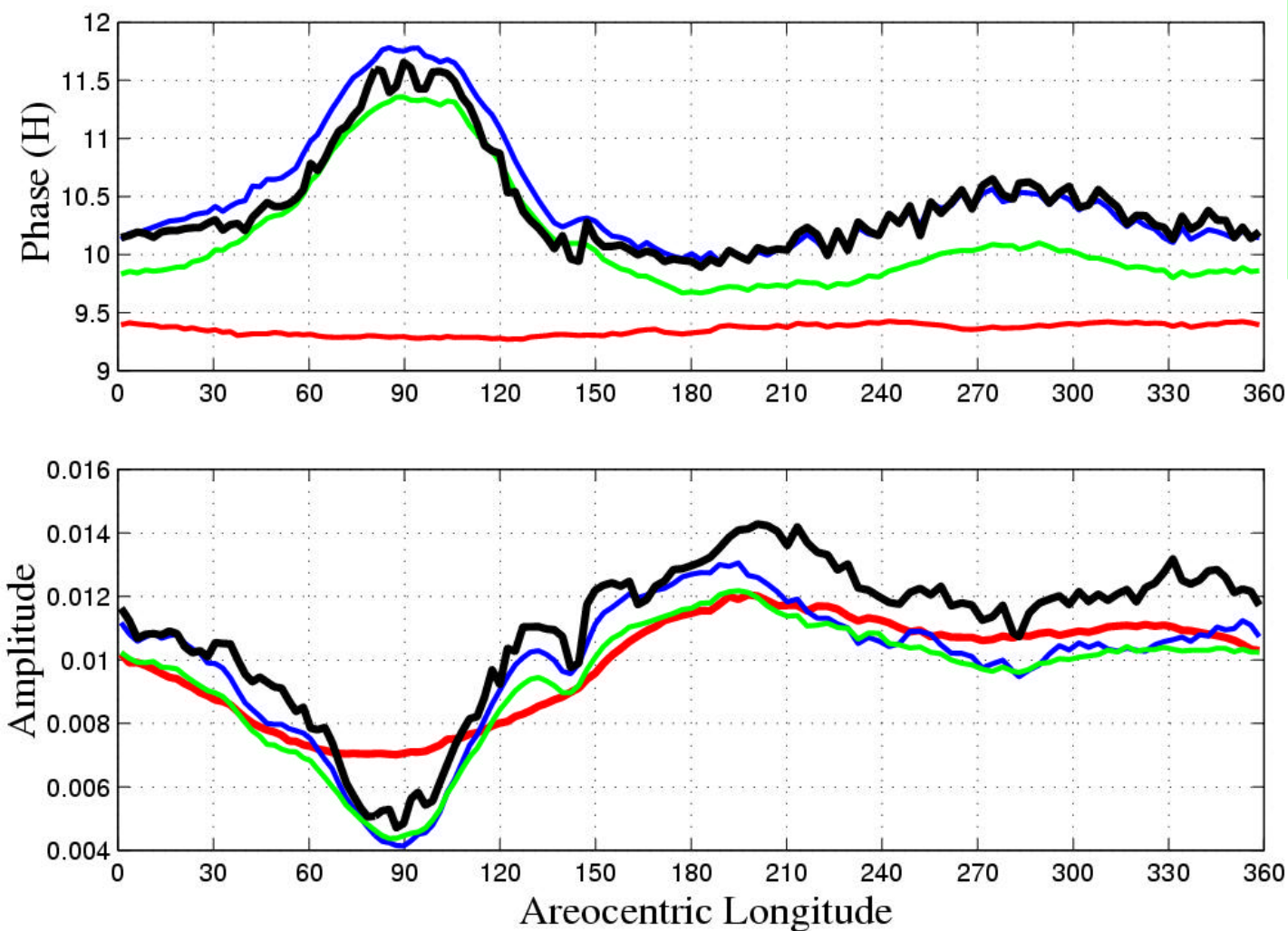
Migrating tide phase is relatively invariant



Longitude

Relatively little variation in migrating tide amplitude over season (~40%)---much larger longitudinal variation.

Simulated Semidiurnal Tide at VL1



--- Simulated VL1

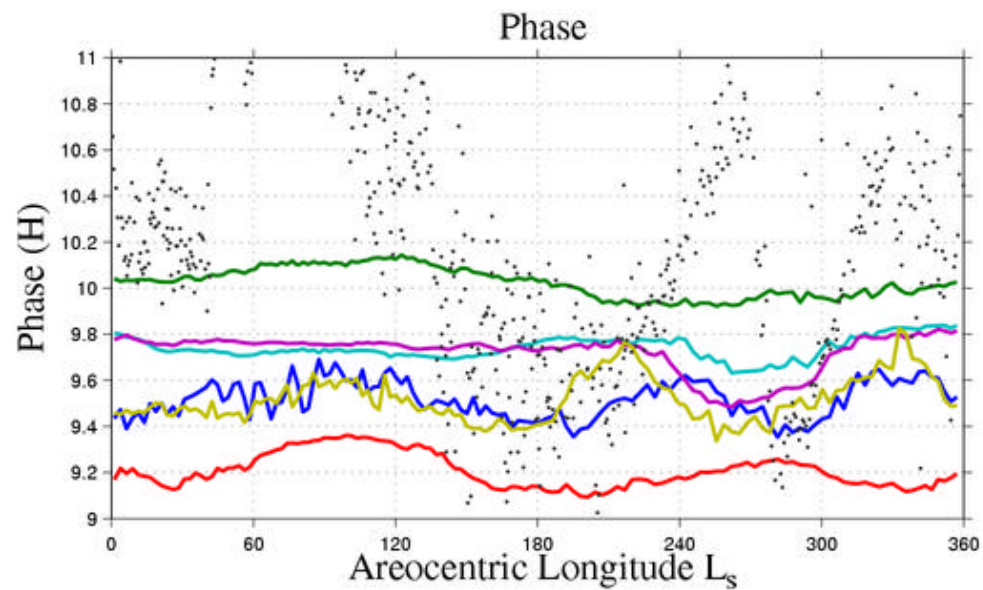
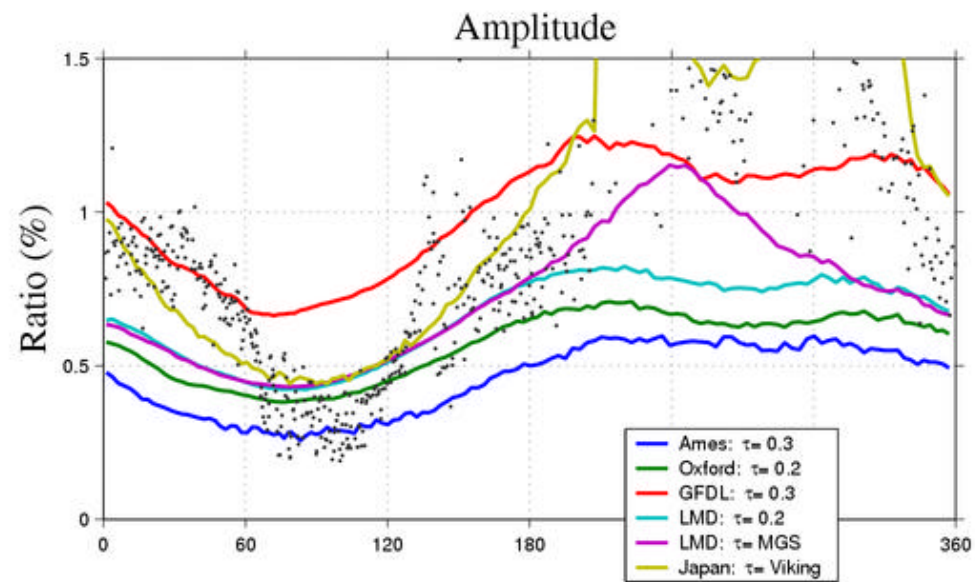
--- $A_{2,2}$ mode only

--- $A_{2,2} + A_{-2,2}$

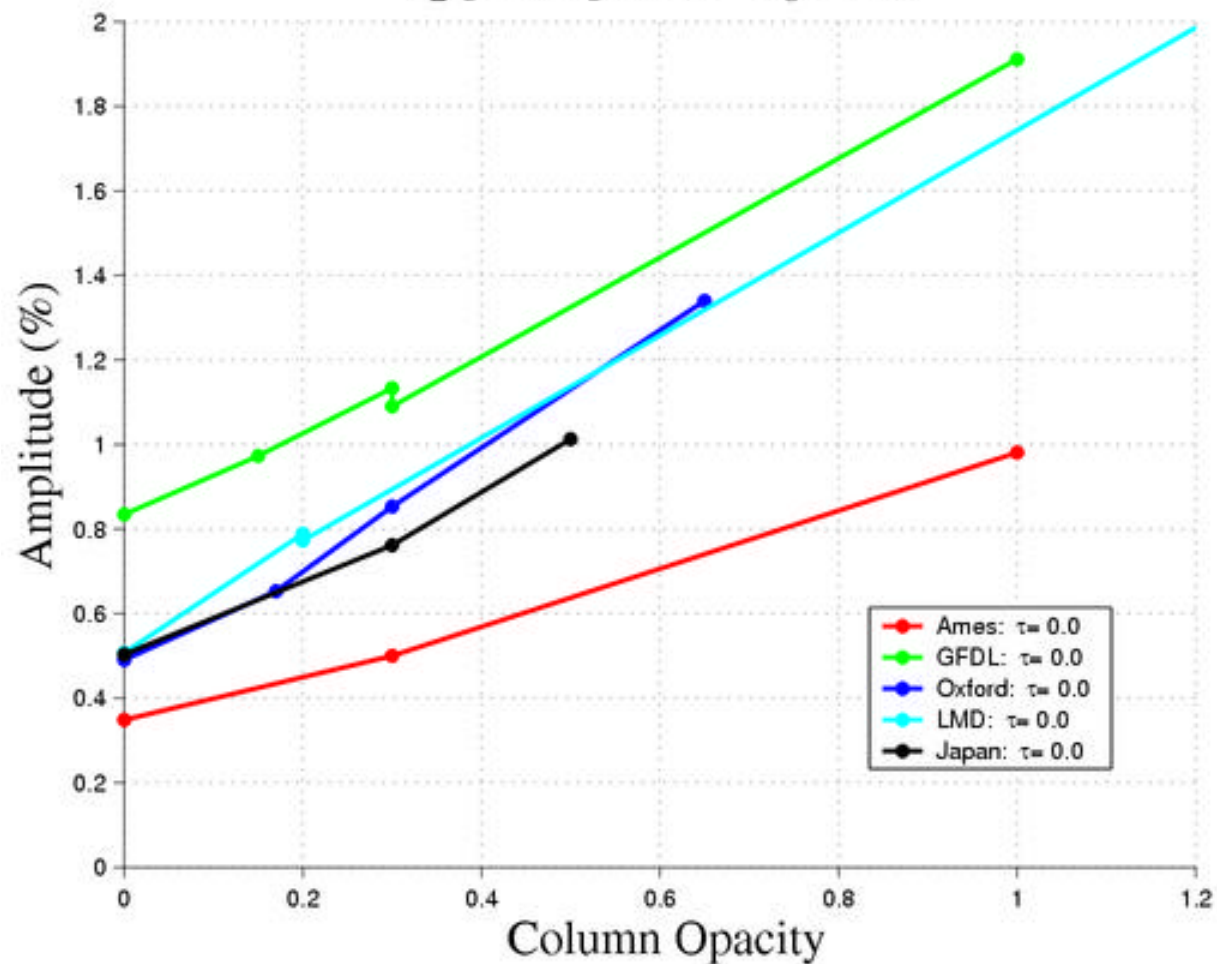
Sun-sync tide
consistent with
seasonally
varying
insolation with
constant dust

Note marked decline in tide amplitude at NH solstice: due to destructive interference by the enhanced Kelvin wave: difference between red and green curves.

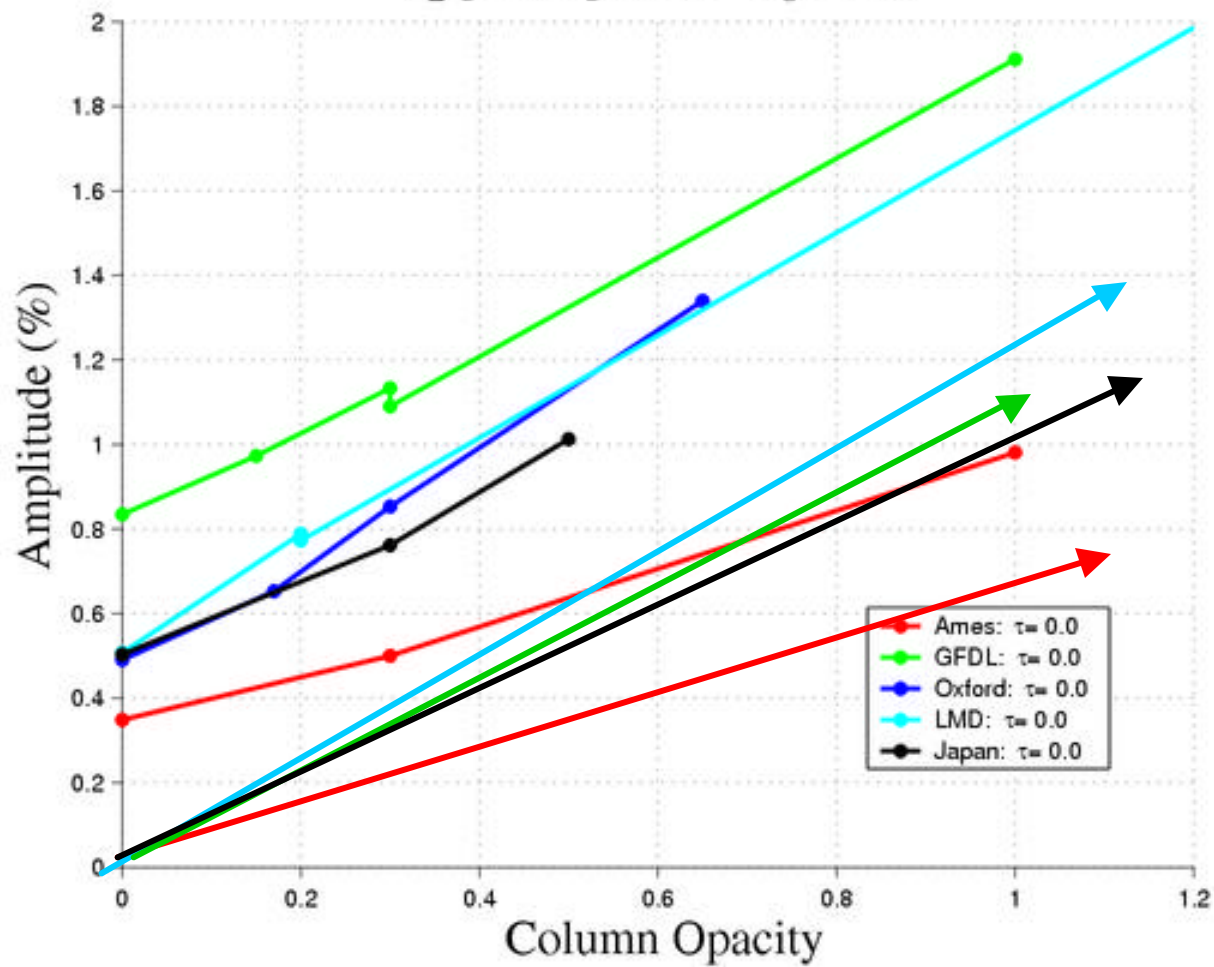
Migrating Semidiurnal Tide: $S_2(p)$: VL1



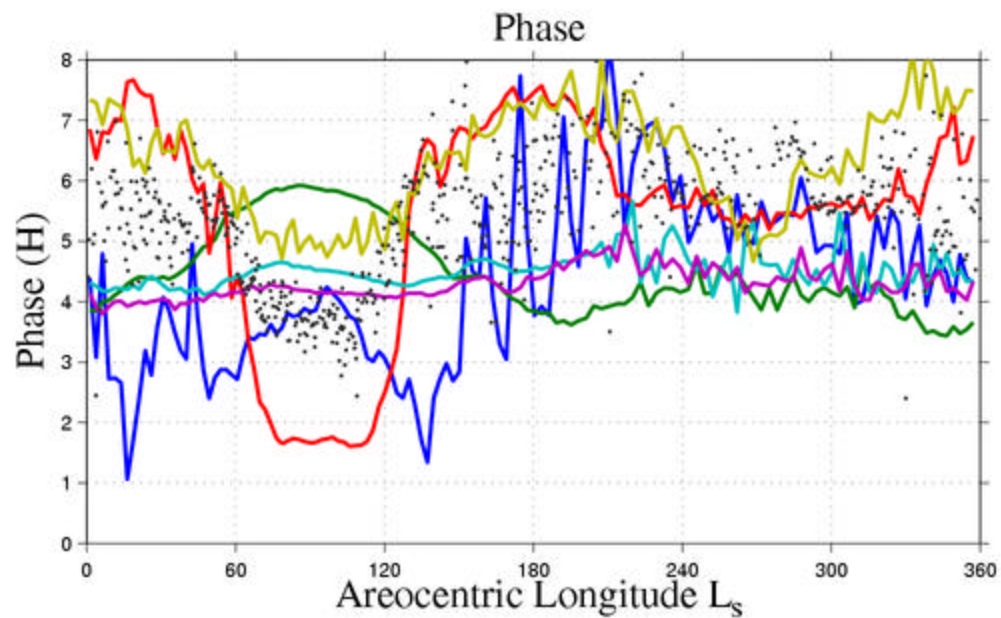
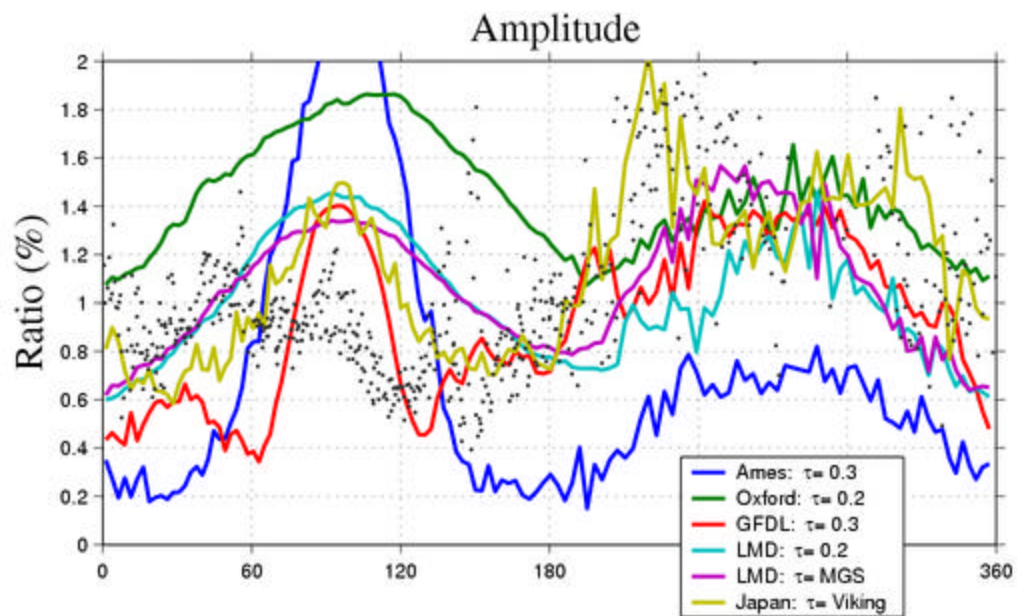
$S_2(p)$ Amplitude $L_s = 180^\circ$



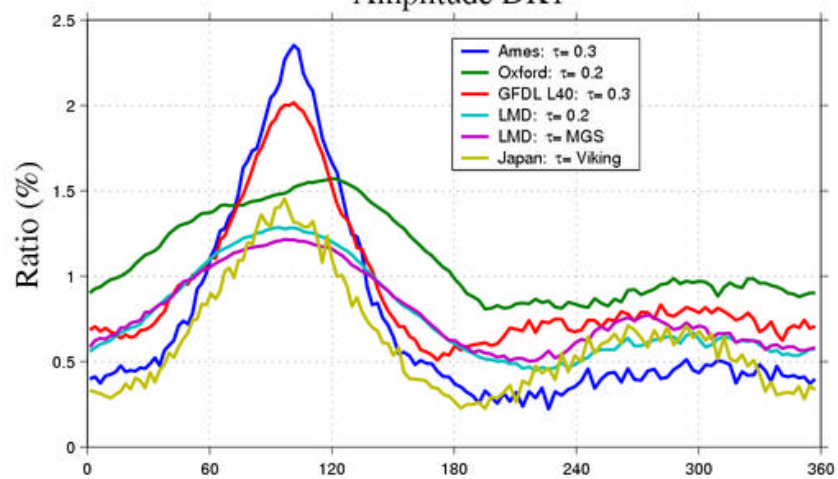
$S_2(p)$ Amplitude $L_s = 180^\circ$



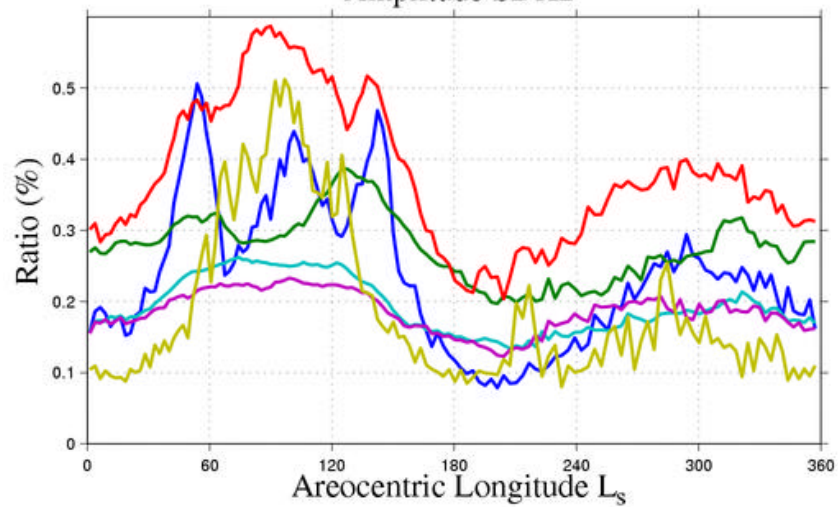
Diurnal Tide: $S_1(p)$: VL1



Amplitude DK1



Amplitude SDK2



Ames $\tau=0.3$ Tides: Lat= 22.5°

